Optimal design accounting for uncertainty in loading amplitudes: a numerical investigation

Bence Balogh[a], Matteo Bruggi[b], Janos Lógó[a]

[a] *Department of Structural Mechanics, Budapest University of Technology and Economics, 1111 Budapest, Hungary*
[b] *Department of Civil and Environmental Engineering, Politecnico di Milano, 20133 Milano, Italy*

Abstract

A numerical investigation is performed addressing the optimal design of stiff structures accounting for uncertainty in loading amplitudes. A minimum volume problem is endowed with a stochastic compliance constraint handling normal distributions and solved adopting mathematical programming. The formulation, originally conceived for a single load case, is extended to handle multiple load cases. Numerical simulations are performed to test the proposed algorithms, pointing out features of the numerical procedures and peculiarities of the stochastic–based optimal solutions achieved for different values of the second order moments. Comparisons with respect to conventional deterministic layouts are provided, as well.

Keywords: robust topology optimization, probabilistic loading conditions, stochastic compliance, multiple load cases

1. Introduction

Topology optimization is a powerful design tool that distributes material on a design domain such that an objective performance is maximized (Maxwell, 1870, Michell, 1904, Bendsøe and Sigmund, 2003). The conventional approach is the so–called minimum compliance formulation

Email addresses: balogh.bence@epito.bme.hu (Bence Balogh), matteo.bruggi@polimi.it (Matteo Bruggi), logo@ep-mech.me.bme.hu (Janos Lógó)

that minimizes the strain energy for an available volume fraction of material (Wasiutynski, 1939, Hemp, 1958, Rossow and Taylor, 1973, Bendsøe and Kikuchi, 1995). Coupling a finite element solver and an optimization algorithm, the stiffest layout can be found that generally consists of a truss–like structure. The results achieved through this original formulation can be directly used to address the preliminary design of devices and mechanical parts, see in particular Bremicker et al. (1991), Zhang et al. (2015), that also provide details on the further processing needed to get the final built design (e.g. interpretation, subsequent shape optimization, detailing). The minimum compliance formulation can be also adopted to visualize optimal stress paths to reinforce structures and structural components, see e.g. recent applications in problems of civil engineering in Bruggi and Taliercio (2015), Bruggi (2016a). Topology optimization is nowadays a mature area of research. Several formulations, solutions methods and applications are available in the literature involving many branches of engineering, see e.g. some recent and comprehensive reviews in Sigmund and Maute (2013), Deaton and Grandhi (2014). Reference is made in particular to the adoption of topology optimization to synthesize optimal mechanisms as investigated e.g. in Sigmund (1997), Saxena and Ananthasuresh (2001), Yin and Ananthasuresh (2003).

Most of the optimization approaches address load, geometry and mechanical parameters as deterministic data, notwithstanding the inherent uncertainty related to the modeling of real–life engineering problems, see e.g. Kim et al. (2006). However, such an important issue has been considered in structural optimization since some pioneering works addressing truss design, see in particular Ben–Tal and Nemirovski (1997) and Marti (2005). Reference is also made to the unified (nonprobabilistic and nonpossibilistic) approach presented in the recent work by Csébfalvi (2014), where varying load directions are handled as uncertain–but–bounded parameters. In topology optimization, two main approaches has been investigated to address the above mentioned sources of uncertainty. Reliability–based optimization methods define limit states and compute the relevant probability failure, whereas the so–called robust design method copes with the stochastic moments

of the system response, see e.g. Schuëller and Jensen (2008) and Tsompanakis et al. (2008). The latter approach has been demonstrated for random loads in Lógó (2007), Guest and Igusa (2008), Lógó et al. (2009) for compliant structures and in Kogiso et al. (2008) for compliant mechanisms. Reference is made e.g. to Lazarov et al. (2012), Chun et al. (2016), da Silva and Cardoso (2017) for extended and up–to–date discussions on the methods available to cope with geometric and material uncertainties.

As introduced in Lógó (2007), the automatic generation of stiff layouts under the effect of loads with uncertain amplitude can be robustly tackled through a minimum weight formulation that enforces a stochastic constraint on the allowed compliance. The evaluation of this constraint is based on the assumption that the loads are affected by uncertainties in their magnitude such that their joint normal distribution function, mean values, and covariances are known. Following Prékopa (1995), if the probability of the compliance value is prescribed as a minimum probability value, the probabilistic constraint can be replaced by an equivalent deterministic one to be implemented in the original minimum weight problem. The original implementation was driven by an ad hoc optimality criterion and did not include any kind of constraint against mesh dependence, whereas the secondary meshing technique was adopted to prevent checkerboard.

The aim of this work is providing a numerical investigation adopting the formulation originally presented in Lógó (2007), which is herein implemented in conjunction with a density filter approach and solved through mathematical programming. Additionally, the formulation is extended to the case of multiple load cases accounting for load conditions that can be either correlated or uncorrelated. Details on the robust and efficient implementation are given, focusing especially on the sensitivity computation. Numerical results point out the effect of uncertainties on the optimal design, showing that load variance has a remarkable effect on the achieved stochastic–based optimal solutions.

The layout of the paper is as follows. Section 2 reviews the original optimization problem

accounting for random forces that all belong to a single load case. It also provides details on the sensitivity analysis performed to feed the minimization algorithm, the Method of Moving Asymptotes (MMA), see Svanberg (1987). Section 3 presents the extension of the original formulation to multiple load cases. Section 4 discusses numerical results comparing the achieved solutions accounting for uncertainty with standard optimal layouts found for deterministic loads. Section 5 resumes the main findings of this contribution, outlining ongoing extensions.

2. The compliance–constrained design problem: single load case

A set of n probabilistic point loads defining a single load case is considered. The i–th force f_i is a random variable with normal distribution and mean value $\bar{f}_i$. The covariance matrix is denoted as $\mathbf{K}_{ov}$, whose components are $k_{i,j}$. In case of uncorrelated loads, $\mathbf{K}_{ov}$ is a diagonal matrix whose terms are the variances of the random variables, i.e. $k_{i,i} = \sigma_i^2$. If the loads are correlated, off-diagonal terms arise to account for the (non–zero) covariances, i.e. $k_{i,j} = \sigma_{ij}$ for $i \neq j$.

The design domain is discretized using a mesh of N displacement–based finite elements. A topology optimization approach is implemented, based on the Solid Isotropic Material with Penalization, see e.g. Bendsøe and Kikuchi (1995). Indeed, a penalization of the material stiffness is provided depending on the value of the minimization unknown, the density field. Denoting by x_e the element–wise constant density entering the conventional SIMP model in the e–th finite element, one has that the element stiffness matrix of the e–th element reads $\mathbf{K}_e(x_e) = x_e^p \, \mathbf{K}_{e0}$, where $\mathbf{K}_{e0}$ element stiffness matrix in case of full material and $p = 3$. According to Lógó (2007),

stiff truss–like models can be generated resorting to the following discrete statement:

$$\begin{cases} \min\limits_{x_{min} \leq x_e \leq 1} & \mathcal{W} = \sum\limits_{e=1}^{N} x_e A_e \\ \text{s.t.} & \mathbf{K}(\mathbf{x})\bar{\mathbf{U}} \ = \ \mathbf{F}(\bar{f}_i), \\ & \sum_{e=1}^{N} \bar{\mathbf{U}}_e^T \ \mathbf{K}_e(x_e) \ \bar{\mathbf{U}}_e - \alpha \mathcal{C}_0 + 2\Phi^{-1}(q)(\mathbf{Y}^T \mathbf{K}_{ov} \mathbf{Y})^{1/2} \leq 0. \end{cases} \tag{1}$$

In the above equation, the objective function is the weight $\mathcal{W}$, which is computed multiplying the element density x_e for the relevant area A_e over the N elements in the mesh. The first constraint enforces the discrete equilibrium of the body when acted upon by the average value of the probabilistic load: $\mathbf{K}$ is the global stiffness matrix, $\bar{\mathbf{U}}$ the global displacement vector computed for the mean values $\bar{f}_i$ and $\mathbf{F}(\bar{f}_i)$ the relevant r.h.s. vector.

Following Prékopa (1995), the second enforcement in Eqn. (1) is used to prescribe the compliance constraint in case of probabilistic loads. It enforces a user–defined lower bound $0 < q < 1$ to the probability that the compliance $\mathcal{C}$ computed for the mean values of the probabilistic loads is lower than a prescribed limit $\alpha \mathcal{C}_0$, i.e.:

$$P\left(\sum_{e=1}^{N} \mathbf{U}_e^T \ \mathbf{K}_e(x_e) \ \mathbf{U}_e - \alpha \mathcal{C}_0 \leq 0 \right) \geq q, \tag{2}$$

where $\mathcal{C}_0$ is herein assumed as the overall compliance found for the full domain made of virgin material ($x_e = 1$ everywhere) enforcing $f_i = \bar{f}_i$, whereas α is a user–defined parameter. The compliance is computed considering the element–wise contributions depending on the element stiffness matrices $\mathbf{K}_e(x_e)$ and the element displacement vectors $\bar{\mathbf{U}}_e$.

It must be remarked that equivalence of Eqn. (2) with the second constraint of Eqn. (1) holds only in case of normal distribution of the load amplitude, as assumed throughout the paper.

However, if a non–Gaussian distribution is given or the data set is probabilistic, an approximation technique could be applied at first. Indeed, the non–Gaussian distribution could be replaced by a surrogate Gaussian model by means of a transformation, see e.g. Bacharoglou (2010).

The second constraint in Eqn. (1) requires the computation of the vector $\mathbf{Y} = [\bar{u}_1 \ ... \ \bar{u}_n]$ that collects, for each one of the n probabilistic loads, the displacement component of the loaded point along the direction of the applied force. For the i–th load, this can be computed as $\bar{u}_i = \mathbf{L}_i^T \bar{\mathbf{U}}$, being $\mathbf{L}_i$ a vector made of null entries except for the degrees of freedom of the loaded node. A horizontal or vertical load requires a unitary value for the degree of freedom corresponding to the displacement along the x-axis or the y-axis, respectively. In case of a load having a general inclination with respect to the reference axes, both degrees of freedom should be equal to one. $\Phi^{-1}(q)$ is the inverse cumulative distribution function of the normal distribution (probit function), evaluated at q.

2.1. Problem implementation

The statement in Eqn. (1) is solved through the gradient–based minimizer MMA (Svanberg, 1987), calling for the computation of the sensitivity at each iteration of the minimization algorithm. The initial guess is the full material domain, that means $x_e = 1$ in each element.

The derivatives of the l.h.s. of the second constraint in Eqn. (1) with respect to the element–wise constant material density x_k read:

$$-\sum_{e=1}^{N} \bar{\mathbf{U}}_e^T \frac{\partial \mathbf{K}_e(x_e)}{\partial x_k} \bar{\mathbf{U}}_e + \Phi^{-1}(q) \frac{\frac{\partial \mathbf{Y}^T}{\partial x_k} \mathbf{K}_{ov} \mathbf{Y} + \mathbf{Y}^T \mathbf{K}_{ov} \frac{\partial \mathbf{Y}}{\partial x_k}}{(\mathbf{Y}^T \mathbf{K}_{ov} \mathbf{Y})^{1/2}}, \tag{3}$$

where the first part is the well–known derivative of the compliance computed for mean values of the forces. In the above equation, the sensitivity of the components of the vector $\mathbf{Y}$ can be efficiently computed through the adjoint method. The term $\bar{u}_i = \mathbf{L}_i^T \bar{\mathbf{U}}$ does not change if one adds

at the right hand side of this equation a zero function that involves the discrete linear equilibrium reported in the first constraint of Eqn. (1), i.e.:

$$\bar{u}_i = \mathbf{L}_i^T \bar{\mathbf{U}} - \boldsymbol{\lambda}^T \left(\mathbf{K}(\mathbf{x}) \bar{\mathbf{U}} \; - \; \mathbf{F}(\bar{f}_i) \right), \tag{4}$$

where $\boldsymbol{\lambda}$ is any arbitrary but fixed vector. After rearrangement of terms and remembering that an element–wise density discretization is adopted, the derivative of $\bar{u}_i$ with respect to the k-th unknown may be computed as:

$$\frac{\partial \bar{u}_i}{\partial x_k} = -\boldsymbol{\lambda}^T \; \frac{\partial \mathbf{K}_e(x_e)}{\partial x_k} \; \bar{\mathbf{U}}_e, \tag{5}$$

where $\boldsymbol{\lambda}$ satisfies the adjoint equation $\mathbf{K}\boldsymbol{\lambda} = \mathbf{L}_i$.

Four–node Serendipity finite elements are used along with an element–wise constant approximation of the density variables. This discrete scheme is well–known to be affected by numerical instabilities such as the arising of undesired checkerboard patterns and mesh dependence, see e.g. Bendsøe and Sigmund (2003), Sigmund and Petersson (1998), Guest et al. (2004). A density filter approach (Bourdin, 2001) is herein adopted instead of applying the filter to the objective function and its sensitivities, as done in most cases. The original design variables x_e are transformed in new sets of physical unknowns $\tilde{x}_e$ reading:

$$\tilde{x}_e = \frac{1}{\sum_N H_{el}} \sum_N H_{el} x_l, \qquad H_{el} = \sum_N \max(0, r_{min} - \mathrm{dist}(e,l)). \tag{6}$$

In the above equation $\mathrm{dist}(e,l)$ is the distance between the centroid of the e–th and l–th element, whereas $r_{min} > d_m$ is the filter radius, being d_m the reference size of the finite elements. The assumption $r_{min} = 1.5 d_m$ is done for all the simulations presented in Section 4 to avoid the arising of checkerboard patterns and to prescribe a minimum thickness to the arising bars. The adopted density–based approach is well–suited to implement, with some modification, recent procedures to

include manufacturing constraints, see in particular Zhou et al. (2015).

3. The compliance–constrained design problem: multiple load cases

This section provides and extension of the formulation in Eqn. (1), assuming not one but n load cases, see Bendsøe et al. (1995). Hence the force f_i is a random variable with normal distribution and mean value $\bar{f}_i$ assigned to the i–th load case. The covariance matrix of the random forces is denoted as $\mathbf{K}_{ov}$. The modified formulation for multiple load cases reads:

$$\begin{cases} \min\limits_{x_{min} \leq x_e \leq 1} & \mathcal{W} = \sum\limits_{e=1}^{N} x_e A_e \\ \text{s.t.} & \mathbf{K}(\mathbf{x})\bar{\mathbf{U}}_i \;=\; \mathbf{F}_i(\bar{f}_i), \quad \text{for } i = 1...n \\ & \sum_{i=1}^{n} \sum_{e=1}^{N} \bar{\mathbf{U}}_{i,e}^T \, \mathbf{K}_e(x_e) \, \bar{\mathbf{U}}_{i,e} - \alpha \mathcal{C}_0 + 2\Phi^{-1}(q)(\mathbf{Y}^T \mathbf{K}_{ov} \mathbf{Y})^{1/2} \leq 0. \end{cases} \tag{7}$$

In the above statement, the first constraint enforces the discrete equilibrium of the body when acted upon by each one of the n probabilistic load cases. Remembering that each load case contains one force only, $\bar{\mathbf{U}}_i$ is the global displacement vector computed for the mean value of the i–th force $\bar{f}_i$, whereas $\mathbf{F}_i(\bar{f}_i)$ is the relevant r.h.s. vector, both addressing the i–th load case.

The second constraint of Eqn. (7) enforces a user–defined lower bound $0 < q < 1$ to the probability that the sum of the compliances computed for the mean values of each one of the n probabilistic load cases is lower than a prescribed limit $\alpha \mathcal{C}_0$., i.e.:

$$P\left(\sum_{i=1}^{n} \sum_{e=1}^{N} \mathbf{U}_{i,e}^T \, \mathbf{K}_e(x_e) \, \mathbf{U}_{i,e} - \alpha \mathcal{C}_0 \leq 0 \right) \geq q, \tag{8}$$

where α is that introduced in the second constraint of Eqn. (1), whereas $\mathcal{C}_0$ is assumed as the sum over the n load cases of the relevant compliances found when the full domain made of virgin

material ($x_e = 1$ everywhere) is loaded by $\bar{f}_i$. For each load case, the compliance is computed considering the element–wise contributions depending on the element stiffness matrices $\mathbf{K}_e(x_e)$ and the relevant element displacement vectors $\bar{\mathbf{U}}_{i,e}$.

The second constraint in Eqn. (7) requires the computation of the vector $\mathbf{Y} = [\bar{u}_1 \ ... \ \bar{u}_n]$ that collects, for each one of the n probabilistic loads, the displacement component of the loaded point along the direction of the applied force in the relevant load case. For the i–th (point) load, this can be equivalently written as $\bar{u}_i = \frac{1}{\bar{f}_i}\mathbf{F}_i^T\bar{\mathbf{U}}_i$. This form will be exploited next in the sensitivity computation.

3.1. Problem implementation

The same implementation described in Section 2.1 will be used. The derivatives of the l.h.s. of the second constraint in Eqn. (7) with respect to the element–wise constant material density x_k read:

$$-\sum_{i=1}^{n}\sum_{e=1}^{N}\bar{\mathbf{U}}_{i,e}^T\,\frac{\partial\mathbf{K}_e(x_e)}{\partial x_k}\,\bar{\mathbf{U}}_{i,e} + \Phi^{-1}(q)\frac{\frac{\partial\mathbf{Y}^T}{\partial x_k}\mathbf{K}_{ov}\mathbf{Y} + \mathbf{Y}^T\mathbf{K}_{ov}\frac{\partial\mathbf{Y}}{\partial x_k}}{(\mathbf{Y}^T\mathbf{K}_{ov}\mathbf{Y})^{1/2}}, \tag{9}$$

where the sensitivity of the components of the vector $\mathbf{Y}$ can be computed through the adjoint method. The term $\bar{u}_i$ does not change if one adds at the right hand side of its statement a zero function that involves the discrete linear equilibrium reported in the first constraint of Eqn. (7), i.e.:

$$\bar{u}_i = \frac{1}{\bar{f}_i}\mathbf{F}_i^T\bar{\mathbf{U}}_i - \boldsymbol{\lambda}^T\left(\mathbf{K}(\mathbf{x})\bar{\mathbf{U}}_i \ - \ \mathbf{F}_i(\bar{f}_i)\right), \tag{10}$$

where $\boldsymbol{\lambda}$ is any arbitrary but fixed vector. After rearrangement of terms and remembering that an element–wise density discretization is adopted, the derivative of $\bar{u}_i$ with respect to the k-th unknown may be computed as:

$$\frac{\partial\bar{u}_i}{\partial x_k} = -\boldsymbol{\lambda}^T\,\frac{\partial\mathbf{K}_e(x_e)}{\partial x_k}\,\bar{\mathbf{U}}_{i,e} = -\frac{1}{\bar{f}_i}\bar{\mathbf{U}}_{i,e}^T\,\frac{\partial\mathbf{K}_e(x_e)}{\partial x_k}\,\bar{\mathbf{U}}_{i,e}, \tag{11}$$

where $\boldsymbol{\lambda}$ satisfies the adjoint equation $\mathbf{K}\boldsymbol{\lambda} = \frac{1}{\bar{f}_i}\mathbf{F}_i$, that means $\boldsymbol{\lambda} = \frac{1}{\bar{f}_i}\bar{\mathbf{U}}_{i,e}$. Differently from Eqn. (5), no additional system of equations must be solved, due to the arising of a self–adjoint problem. Indeed, Eqn. (5) turns out to be a self–adjoint problem only if a single point force is considered in the optimization.

It is finally remarked that both problems in Eqn. (1) and Eqn. (7) are conceived to handle load cases including point forces only. However, introducing some simplifications, distributed loads with uncertainty in loading amplitude could be handled as well. For instance, a uniformly distributed load could be implemented in the discrete framework as a set of equivalent point forces that share a normal distribution with equal mean value and variance, being part of the same i–th load or load case in Eqn. (1) or in Eqn. (7), respectively. The computation of the overall compliance would not be affected by this change, whereas the vector $\mathbf{Y}$ should collect, for each one of the probabilistic distributed loads, the displacement components of the loaded points along the direction of the relevant equivalent point force. Of course, the matrix $\mathbf{K}_{ov}$ should be populated with variances and covariances of the distributed loads accordingly.

4. Numerical simulations

A numerical investigation is performed in this section to assess the formulation for single load case in Eqn. (1) and that for multiple load cases in Eqn. (7), pointing out peculiar features of the optimal layouts achieved accounting for uncertainty in loading amplitudes.

Geometry and boundary conditions of the considered examples are those represented in Figure 1. Non–dimensional parameters are used to feed the algorithm. A unitary Young modulus is used, whereas the Poisson's ratio reads $\nu = 0.2$. Unitary thickness is assumed for the specimens. A mesh with 8192 bi–linear square elements is adopted for Example 1, whereas the L–shaped corbel of Example 2 is handled by means of 12288 elements.

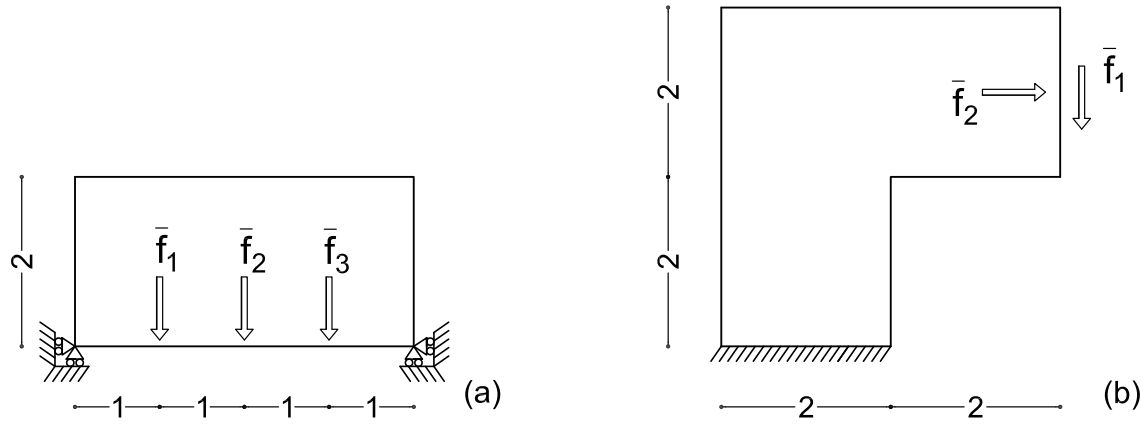

Figure 1: Geometry and boundary conditions. Example 1 (a) and Example 2 (b).

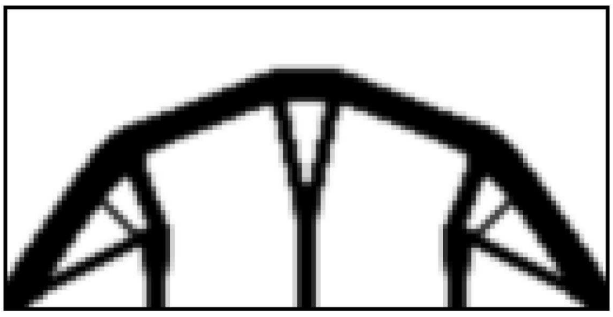

Figure 2: Example 1. Single load case. Optimal design in case of deterministic loads ($\mathcal{W} = 22.87$).

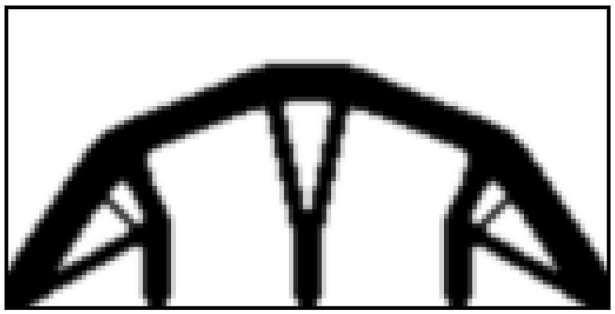

(a)

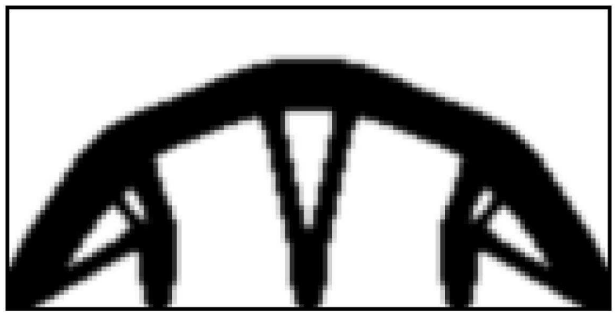

(b)

Figure 3: Example 1. Single load case. Optimal design in case of probabilistic uncorrelated loads with $\sigma_1^2 = \sigma_2^2 = \sigma_3^2 = 1$: $q = 0.95$ (a - $\mathcal{W} = 27.22$) and $q = 0.9999$ (b - $\mathcal{W} = 33.35$).

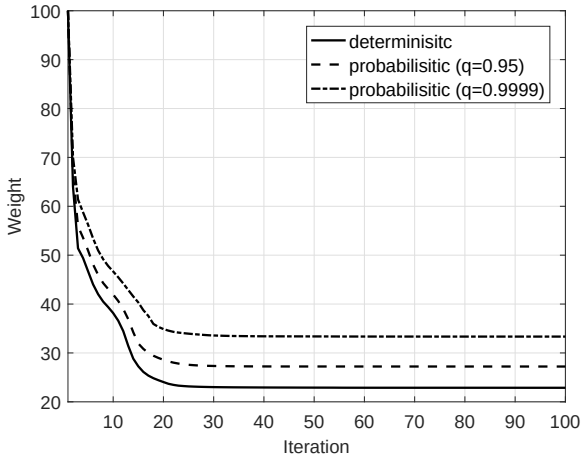

Figure 4: Example 1. Single load case. History plot of the objective function for the considered optimization problems.

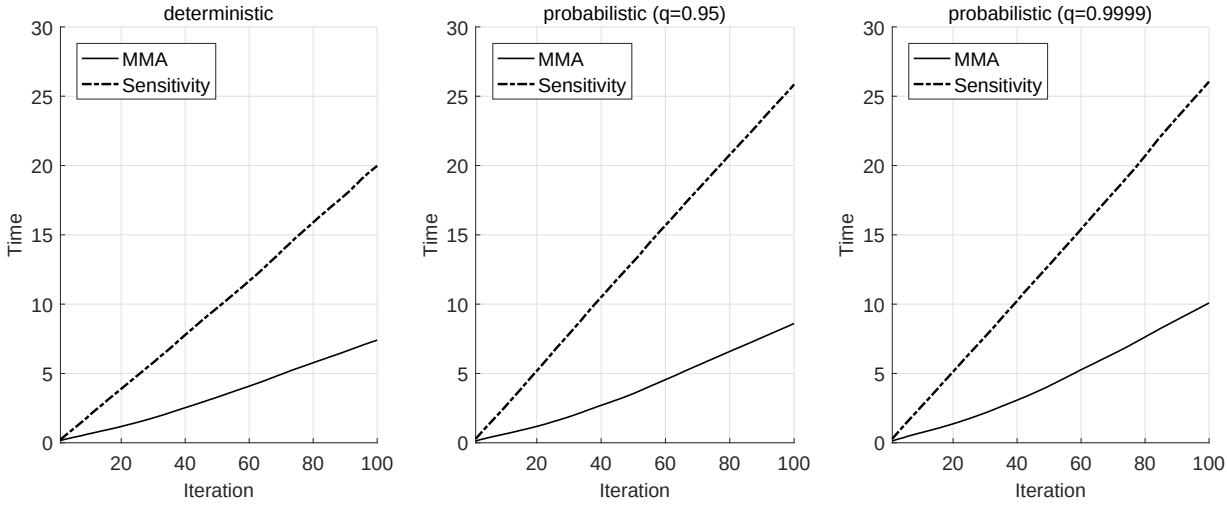

Figure 5: Example 1. Single load case. CPU time (seconds) to run the considered optimization problems.

4.1. Example 1 - single load case

The example originally presented in Lógó (2007) is considered to test the formulation in Eqn. (1). The design domain is a lamina with aspect ratio 4:2 that is fixed at the ground through two hinges located at the corners of the lower side, see Figure 1(a). Three vertical forces are considered acting simultaneously (within the same load case) with average values $\bar{f}_1 = \bar{f}_2 = \bar{f}_3 = 10$, being $n = 3$.

At first, a conventional compliance-constrained minimum weight design is investigated, assuming that the force amplitude is deterministic (with prescribed value equal to the average one). The compliance constraint is used to distribute the minimum amount of material such that the strain energy stored by the optimal structure is not larger than α times the energy stored in the whole design domain acted upon by the same load case. The prescription $\alpha = 2.5$ holds for all the numerical examples investigated in this section. The achieved optimal design is shown in Figure 2, whose caption reports the relevant weight, being $\mathcal{W} = 100$ the weight of the whole design domain. The achieved result is in good agreement with the analytical solution originally derived in Chan

(1963), as already observed in Lógó (2007).

The same example is then investigated accounting for uncertainty in loading amplitudes and assuming uncorrelated loads with variance equal to 10% of the average value, i.e. $\sigma_1^2 = \sigma_2^2 = \sigma_3^2 = 1$. A first numerical investigation is performed to enforce that the compliance $\mathcal{C}$ computed for the mean values does not exceed the prescribed limit $\alpha\mathcal{C}_0$ with, at least, probability $q = 0.95$. The achieved result is shown in Figure 3(a). As already observed in Lógó (2007) for $q = 0.91$, the stochastic constraint requires additional material and some modification in the optimal layout, if compared to the conventional design achieved in case of deterministic loads. In the stochastic–based design the arch is thicker to match any variation of the funicular polygon due to the uncertainty in the uncorrelated values of the amplitude of the three forces and preserve the required stiffness. Also, the sub–structure hanging the central load is larger and heavier. Allowing for a probability of failure equal to 5% calls for an additional 20% of material with respect to the deterministic case.

Figure 3(b) shows the optimal design achieved for $q = 0.9999$, that means that the probability that a failure of the compliance constraint occurs is now reduced to 10^{-4}. The comments already formulated for Figure 3(a) are emphasized when addressing the optimal design achieved for the stricter probabilistic constraint. This design calls for an additional 45% of material with respect to the deterministic case.

Figure 4 shows history plots of the objective function of the formulation in Eqn. (1), referring to the three simulations presented above. A convergence criterion was used to stop the algorithm for a maximum relative difference of the density unknowns between two subsequent iterations equal to 0.001, enforcing a minimum number of iterations equal to 100. As shown in the graph, the two curves referring to the stochastic approach are as smooth as that of the conventional deterministic optimization. Both of them converge to an horizontal plateau after a few tens of steps, independently on the value of the prescribed probability q.

Figure 5 provides a comparison of the computational effort needed to perform the three op-

timization routines discussed above. At each iteration, the objective function, the compliance constraint and its sensitivity are evaluated based on the current value of the minimization unknowns. The gradient–based minimizer processes this information and provides an updated set of density variables. The plots in Figure 5 present the evolution of the CPU time (seconds) spent in the sensitivity computation performed according to Eqn. (3) and in the update of the density unknowns through the optimization algorithm (MMA). The values read on the curves for the last iteration provide the total amount of time spent to handle the sensitivity computation and to perform MMA.

The deterministic compliance constraint gives rise to a self–adjoint problem, see e.g. Bendsøe and Sigmund (2003), meaning that at each iteration of the optimization algorithm a single solution of the state equation is needed to compute both the current value of the compliance and its sensitivity. When dealing with the stochastic constraint in case of the single load case formulation, the solution of additional n adjoint problems of the type in Eqn. (5) is needed, calling for an increased computational cost. However, since all of them share the same stiffness matrix governing the state equation, see Eqn. (3), the factorization of $\mathbf{K}(x)$ is performed at each step to speed up the computation. For the considered example the additional time required for the sensitivity computation by the stochastic formulation is approximately 30% higher than the deterministic one, no matter the value of q.

Looking at the CPU time spent in the minimization algorithm, it can be observed that a slight increase is paid in case of the stochastic constraint, especially for $q = 0.9999$. This is essentially due to the constant $\Phi^{-1}(q)$ that scales the last term of the l.h.s. in the second constraint of Eqn. (1). Indeed, for big values of q the left hand side of the inequality tends to blow up, depending on the inverse cumulative distribution function of the normal distribution.

4.2. Example 1 - multiple load cases

The example presented in Section 4.1 is herein investigated to assess the formulation for multiple load cases in Eqn. (7). A single load case is defined for each one of three vertical forces shown in Figure 1(a) ($n = 3$). As before, the average values of the forces are $\bar{f}_1 = \bar{f}_2 = \bar{f}_3 = 10$.

At first, the force amplitude is assumed to be deterministic. The optimization problem has the aim of distributing the minimum amount of material such that the sum of the strain energies stored by the optimal structure for each force (herein load case) is not larger than α times the sum of the energies computed for the whole design domain. This approach is fully along the lines of the volume–constrained minimization of the weighted sum of the compliances that is conventionally used to deal with more than one load case, see e.g. Bendsøe and Sigmund (2003). The achieved result is a stiff topology that can support not only the loads acting separately, but also any combination of them, see Figure 6.

Then, the same example is investigated accounting for uncorrelated loads with variance equal to 10% of the average value, i.e. $\sigma_1^2 = \sigma_2^2 = \sigma_3^2 = 1$. A first numerical investigation is performed to enforce that the weighted compliance $\mathcal{C}$ computed for the mean values of the loads does not exceed the prescribed limit $\alpha\mathcal{C}_0$ with, at least, probability $q = 0.95$. The achieved result is shown in Figure 7(a). As expected, the weight of the optimal solution increases (about 15%) with respect to the deterministic case. All the members are thicker, especially the central part of the arch that has a different design.

Reducing to 10^{-4} the maximum probability of failure allowed by the stochastic compliance constraint, i.e. enforcing $q = 0.9999$ in the second constraint of Eqn. (7), the optimal design presented in Figure 7(b) arises. This solution is remarkably different from the layout shown in Figure 7(a). Contrary to expectations after the results achieved in Section 4.1 on the same example, a uniform thickening of all the members is not enough to cope with the stricter stochastic constraint. The central part of the layout in Figure 7(b) resembles that of Figure 7(a), but the

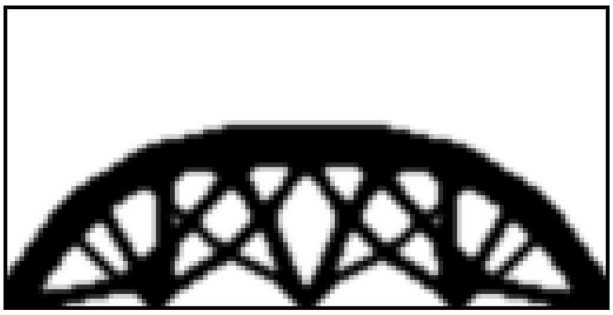

Figure 6: Example 1. Multiple load cases. Optimal design in case of deterministic loads ($\mathcal{W} = 30.77$).

outer parts are much stiffer since no hole is allowed in the massive element. The increase in terms of material with respect to the deterministic case is around 30%.

As already done in Section 4.1, history plots of the objective function referring to the above simulations are compared in Figure 8. The same convergence criterion was used to perform the numerical investigations, except for the minimum number of iterations that was increased to 150. Smooth curves suggest that the adoption of the stochastic constraint does not introduce any numerical issue, independently on the value of q.

A final comparison is provided in terms of CPU times needed to run the algorithm, as reported in Figure 9. Differently from Eqn. (5), no additional system of equations must be solved, due to the arising of a self–adjoint problem in Eqn. (11). However, the handling of the stochastic constraint calls for an extra–time to perform the sensitivity computation with respect to the deterministic case. Again, a slight increase in the CPU time spent in the minimization algorithm is observed for $q = 0.9999$ because of the probit function.

4.3. Example 2 - multiple load cases

A final set of investigations is performed addressing the L–shaped corbel shown in Figure 1(b). Two load cases are defined, i.e. $n = 2$: the first includes a vertical force whereas the second a horizontal one. Their average values are $\bar{f}_1 = \bar{f}_2 = 10$.

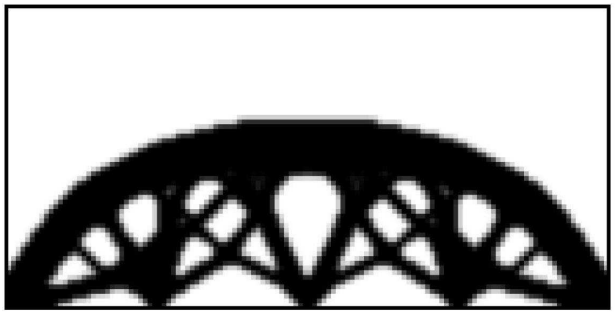

(a)

(b)

Figure 7: Example 1. Multiple load cases. Optimal design in case of probabilistic uncorrelated loads with $\sigma_1^2 = \sigma_2^2 = \sigma_3^2 = 1$: $q = 0.95$ (a - $\mathcal{W} = 35.31$) and $q = 0.9999$ (b - $\mathcal{W} = 40.86$).

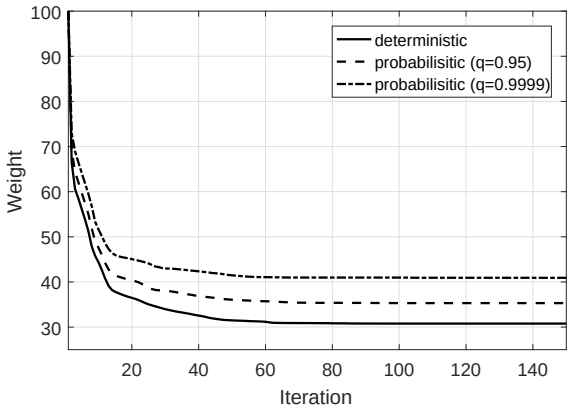

Figure 8: Example 1. Multiple load cases. History plot of the objective function for the considered optimization problems.

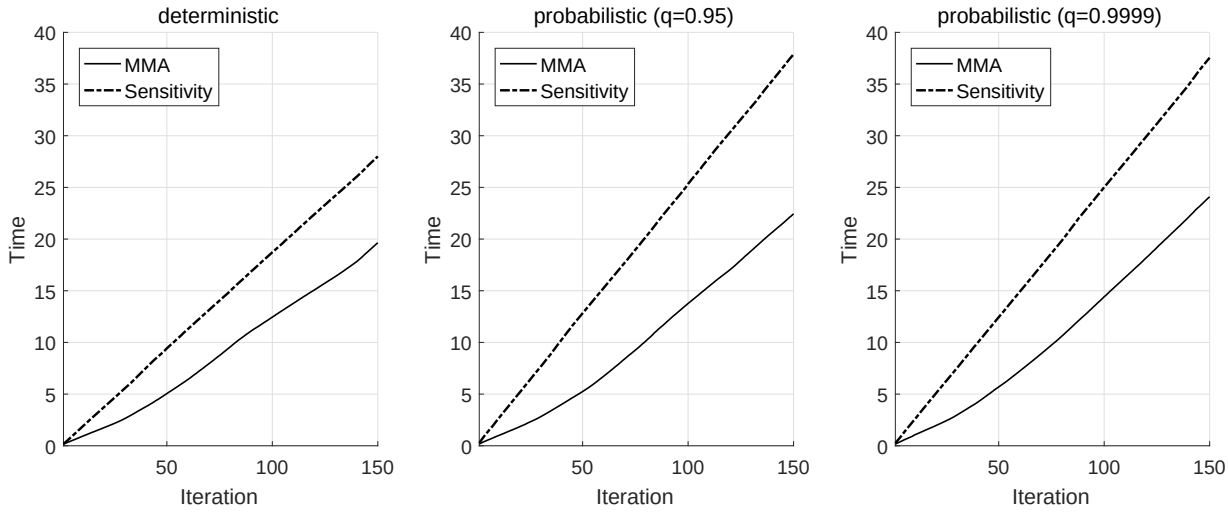

Figure 9: Example 1. Multiple load cases. CPU time (seconds) to run the considered optimization problems.

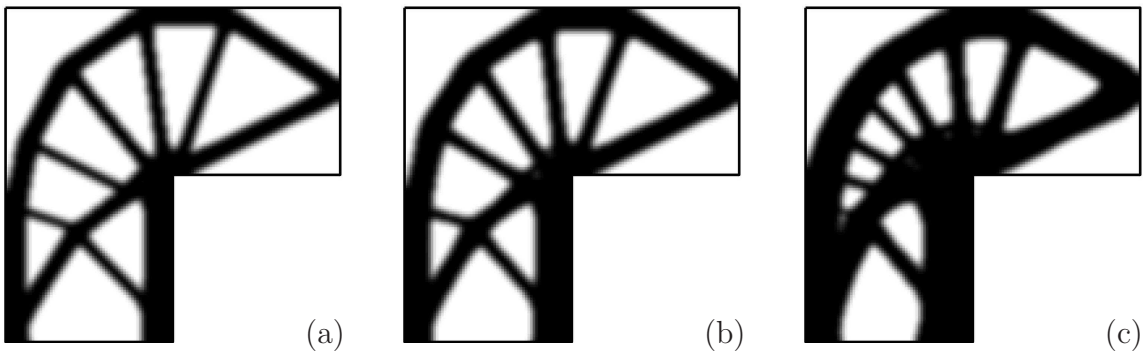

Figure 10: Example 2. Multiple load cases. Optimal design in case of deterministic loads with: $\alpha = 2.5$ (a - $\mathcal{W} = 37.68$), $\alpha = 2.0$ (a - $\mathcal{W} = 45.04$) and $\alpha = 1.5$ (c - $\mathcal{W} = 58.66$).

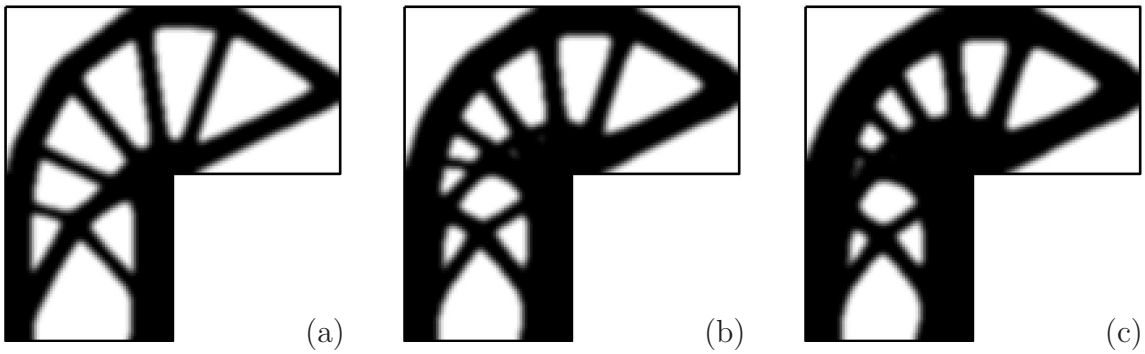

Figure 11: Example 2. Multiple load cases. Optimal design in case of probabilistic uncorrelated loads with $\sigma_1^2 = 1$ $\sigma_2^2 = 1$ ($\alpha = 2.5$): $q = 0.95$ (a - $\mathcal{W} = 46.54$), $q = 0.9999$ (b - $\mathcal{W} = 56.48$) and $q = 0.999999$ (c - $\mathcal{W} = 61.44$).

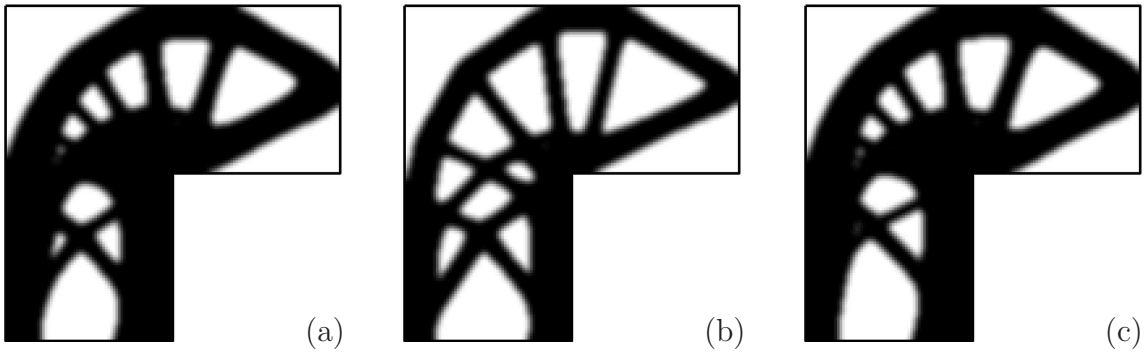

Figure 12: Example 2. Multiple load cases. Optimal design in case of probabilistic uncorrelated loads ($\alpha = 2.5$, $q = 0.95$): $\sigma_1^2 = 10$ $\sigma_2^2 = 10$ (a - $\mathcal{W} = 63.61$), $\sigma_1^2 = 1$ $\sigma_2^2 = 10$ (b - $\mathcal{W} = 51.32$) and $\sigma_1^2 = 10$ $\sigma_2^2 = 1$ (c - $\mathcal{W} = 61.35$).

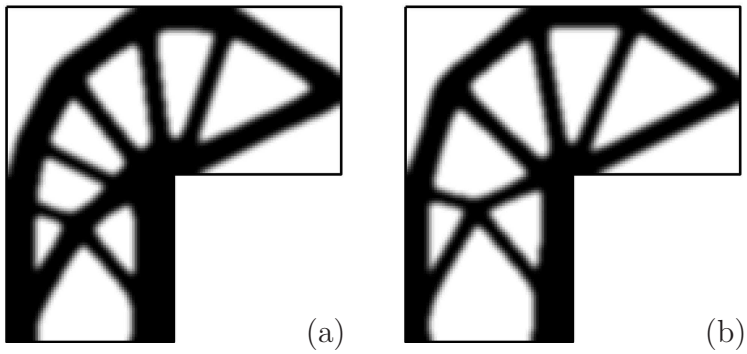

Figure 13: Example 2. Multiple load cases. Optimal design in case of probabilistic correlated loads with $\sigma_1^2 = 1$ $\sigma_2^2 = 1$ ($\alpha = 2.5$, $q = 0.95$): covariance $\sigma_{12} = \sigma_{21} = 1$ (a - $\mathcal{W} = 48.97$) and covariance $\sigma_{12} = \sigma_{21} = -1$ (b - $\mathcal{W} = 42.09$).

Figure 10 shows the optimal layouts achieved in case of deterministic loads for different values of the parameter α governing the compliance constraint. For lower values of α an increased stiffness is required, thus calling for heavier optimal layouts. Figure 10(a) shows the light truss–like structure arising for $\alpha = 2.5$, whereas Figure 10(c) refers to the more branched design of the Michell–like solution found for $\alpha = 1.5$.

The formulation in Eqn. (7) is adopted to enforce the stochastic compliance constraint accounting for $\sigma_1^2 = \sigma_2^2 = 1$ and different values of the allowed probability of failure. The parameter $\alpha = 2.5$ is assigned. For $q = 0.95$, the same topology found for the deterministic design shown in Figure 10(a) arises whereas the thickness of the members grows, see Figure 11(a). For larger values of q, heavier optimal layouts arise that also resort to an increased number of members, see Figure 11(b–c). These stochastic–based solutions preserve a cross–shaped reinforcing structure in the lower part of the corbel that is remarkably different with respect to a deterministic design of similar weight, see Figure 10(c). Indeed, this allows handling effectively the expected variations in the amplitude of the uncorrelated loads independently on the value of q.

An additional set of numerical investigations is performed assuming $\alpha = 2.5$, $q = 0.95$ and different values of the variance of the loads. Figure 12(a) refers to the case $\sigma_1^2 = \sigma_2^2 = 10$, for which an optimal design arises that is very similar to that found for lower variance but larger q, see Figure 11(c). Figures 12(b–c) show that the optimal design is sensitive to the assumption of unequal variances of the loads. An ad hoc cross–shaped reinforcing structure handles the prevailing variance of the horizontal force, see Figure 12(b), whereas the optimal layout in Figure 12(c) is conceived to handle the main uncertainty affecting the vertical load.

The algorithm presented in Section 3 can handle correlated loads, as well. Again, the variances are such that $\sigma_1^2 = \sigma_2^2 = 1$, whereas $\alpha = 2.5$ and $q = 0.95$. A positive covariance, e.g. $\sigma_{12} = \sigma_{21} = 1$, means that greater values of the vertical force mainly correspond to the greater values of the horizontal force. Conversely, for a negative covariance, e.g. $\sigma_{12} = \sigma_{21} = -1$, greater values of

the vertical load mainly correspond with the lesser values of the horizontal load. For positive covariance, a slightly heavier version of the design found in Figure 11(a) for uncorrelated loads is achieved, see Figure 13(a). For negative covariance, a different and lighter design arises that consists of a reduced number of trusses, see Figure 13(b).

5. Conclusions and perspectives

A numerical method has been adopted to cope with the optimal design of stiff structures accounting for uncertainty in loading amplitudes. The compliance–constrained minimum volume approach proposed by Lógó (2007) has been implemented adopting mathematical programming along with a density filter to control mesh dependence and checkerboard. Additionally, the formulation has been extended to handle multiple load cases. The sensitivity computation has been provided for the single load case formulation and the multiple load cases approach. According to Prékopa (1995), the proposed numerical methods hold for loads whose amplitude can be described by a normal distribution.

Numerical simulations have been performed to test both the algorithms, pointing out features of the numerical procedures and peculiarities of the stochastic–based optimal layouts. Referring to numerical issues, smooth convergence is reported along with an acceptable increase of CPU times with respect to the conventional deterministic approach. Optimal results are pure 0–1 solutions and no grey region is found at convergence, except that arising at the boundary of the optimal design because of the adopted density filter. The implemented algorithms are robust with respect to the enforced maximum probability of failure assigned through the compliance constraint. Simulations refer to the range 0.05 - 10^{-6}.

As already found in Lógó (2007) for uncorrelated loads with variance equal to ten percent of their average value, stochastic–based design are, in general, heavier variations of the deterministic layouts. The same outcome arises from the results presented in Section 4.1 for the single load

case formulation, which has been herein investigated for different values of the enforced maximum probability of failure.

With respect to the single load case formulation, the layouts achieved through the formulation for multiple load cases can be more sensitive to the stochastic constraint even for moderate values of the variance of the loads, see Section 4.2. Section 4.3 assesses the role played by the parameters involved in the herein considered stochastic–based formulation, pointing out peculiarities of the probabilistic layouts with respect to deterministic topologies achieved upon request of increased stiffness. In particular, it is shown that the topology of the optimal stochastic–based design can be remarkably affected by the enforced probability of failure for the compliance constraint and the handling of loads with big variances or unequal variances. Also, the effect of positive and negative correlation has been shown to affect at least the weight of the optimal layouts.

The proposed investigations are intended as a numerical study assessing the stochastic compliance constraint within a minimum weight formulation. The ongoing research is mainly devoted to the extension of the proposed formulation to handle stress constraints under the effect of probabilistic loads, see e.g. the multi–constrained minimum weight formulation implemented in Bruggi (2016b).

Acknowledgment

The authors wish to thank the research program OTKA 119440 2016–2020 "Selected problems in structural topology optimization: from basic theory to engineering applications" founded by the National Research, Development and Innovation Office, Hungary

Bacharoglou, A.G. (2010). Approximation of probability distributions by convex mixtures of gaussian measures. *Proceedings of the American Mathematical Society* 138(7):2619–2628. doi:10.1090/S0002-9939-10-10340-2

Bendsøe, M. P., Diaz, A. R., Lipton, R., Taylor, J. E. (1995). Optimal design of material properties and material distribution for multiple loading conditions. *International Journal for Numerical Methods in Engineering* 38(7):1149-1170. doi:10.1002/nme.1620380705

Bendsøe, M. P., Kikuchi, N. (1988). Generating optimal topologies in structural design using a homogenization method. *Computer Methods in Applied Mechanics and Engineering* 71(2):197–224. doi:10.1016/0045-7825(88)90086-2

Bendsøe, M., Sigmund, O., (2003). Topology Optimization - Theory, Methods and Applications. Springer, Berlin.

Ben–Tal, A., Nemirovski, A. (1997). Robust truss topology design via semidefinite programming. *SIAM Journal on Optimization* 7(4):991-1016. doi:10.1137/S1052623495291951

Bourdin, B. (2001). Filters in topology optimization. *International Journal for Numerical Methods in Engineering* 50(9):2143-2158. doi:10.1002/nme.116

Bremicker, M., Chirehdast, M., Kikuchi, N., Papalambros, P. Y. (1991). Integrated topology and shape optimization in structural design. *Mechanics of Structures and Machines* 19(4):551–587. doi:10.1080/08905459108905156

Bruggi, M. (2016). A numerical method to generate optimal load paths in plain and reinforced concrete structures. *Computers and Structures* 170:26-36. doi:10.1016/j.compstruc.2016.03.012

Bruggi, M. (2016). Topology optimization with mixed finite elements on regular grids. *Computer Methods in Applied Mechanics and Engineering* 305:133-153. doi:10.1016/j.cma.2016.03.010

Bruggi, M., Taliercio, A. (2015). Optimal strengthening of concrete plates with unidirectional fiber-reinforcing layers. *International Journal of Solids and Structures* 67-68:311–325. doi:10.1016/j.ijsolstr.2015.04.033

Chan, H. S. Y. (1963). Optimal Michell frameworks for three parallel forces, Report No. 167. Canfield: College of Aeronautics.

Chun, J., Song, J., Paulino, G. H. (2016). Structural topology optimization under constraints on instantaneous failure probability. *Structural and Multidisciplinary Optimization* 53(4):773-799. doi:10.1007/s00158-015-1296-y

Csébfalvi, A. (2014). A new theoretical approach for robust truss optimization with uncertain load directions. *Mechanics Based Design of Structures and Machines* 42(4):442–453. doi:10.1080/15397734.2014.880064

da Silva, G. A., Cardoso, E. L. (2017). Stress-based topology optimization of continuum structures under uncertainties. *Computer Methods in Applied Mechanics and Engineering* 313:647–672. doi:10.1016/j.cma.2016.09.049

Deaton, J. D., Grandhi, R. V. (2014). A survey of structural and multidisciplinary continuum topology optimization: Post 2000. *Structural and Multidisciplinary Optimization* 49(1):1–38. doi:10.1007/s00158-013-0956-z

Guest, J. K., Igusa, T. (2008). Structural optimization under uncertain loads and nodal locations. *Computer Methods in Applied Mechanics and Engineering* 198(1):116–124. doi:10.1016/j.cma.2008.04.009

Guest, J. K., Prévost, J. H., Belytschko, T. (2004). Achieving minimum length scale in topology optimization using nodal design variables and projection functions. *International Journal for Numerical Methods in Engineering* 61(2):238-254. doi:10.1002/nme.1064

Hemp, W. S. (1958). Theory of Structural Design, NATO Studies, Report No. 214, Paris.

Kim, C., Wang, S., Kang, E., Lee, K. (2006). New design process for reliability-based topology optimization of a laser scanned model. *Mechanics Based Design of Structures and Machines* 34(3):325–347. doi:10.1080/15397730600925615

Kogiso, N., Ahn, W., Nishiwaki, S., Izui, K., Yoshimura, M. (2008). Robust topology optimization for compliant mechanisms considering uncertainty of applied loads. *Journal of Advanced Mechanical Design, Systems, and Manufacturing* 2(1):96107 doi:doi.org/10.1299/jamdsm.2.96

Lazarov, B. S., Schevenels, M., Sigmund, O. (2012). Topology optimization considering material and geometric uncertainties using stochastic collocation methods. *Structural and Multidisciplinary Optimization* 46(4):597-612. doi:10.1007/s00158-012-0791-7

Lógó, J. (2007). New type of optimality criteria method in case of probabilistic loading conditions. *Mechanics Based Design of Structures and Machines* 35(2):147–162. doi:10.1080/15397730701243066

Lógó, J., Ghaemi, M., Rad, M. M. (2009). Optimal topologies in case of probabilistic loading: The influence of load correlation. *Mechanics Based Design of Structures and Machines* 37(3):327–348. doi:10.1080/15397730902936328

Marti, K. (2005). Stochastic Optimization Methods. Springer–Verlag, Berlin.

Maxwell, J.C. (1870). On Reciprocal Figures, Frames, and Diagrams of Forces. *Transactions of the Royal Society of Edinburgh* 26(1):1–40.

Michell, A.G.M. (1904). The Limits of Economy of Material in Frames Structures. *Philosophical Magazine* 8:589–597.

Saxena, A., Ananthasuresh, G. K. (2001). Topology optimization of compliant mecha-

nisms with strength considerations. *Mechanics of Structures and Machines* 29(2):199-221. doi:10.1081/SME-100104480

Sigmund, O. (1997). On the design of compliant mechanisms using topology optimization. *Mechanics of Structures and Machines* 25(4):493-524. doi:10.1080/08905459708945415

Sigmund, O., Petersson, J. (1998). Numerical instabilities in topology optimization: A survey on procedures dealing with checkerboards, mesh–dependencies and local minima. *Structural Optimization* 16(1), 68-75.

Prékopa, A. (1995). Stochastic Programming. Budapest, Dordrecht: Akadémia Kiad´ and Kluwer.

Rossow, M. P., Taylor, J. E. (1973). A Finite Element Method for the Optimal Design of Variable Thickness Sheets. *AIAA Journal* 11:1566-1569.

Schuëller, G. I., Jensen, H. A. (2008). Computational methods in optimization considering uncertainties - an overview. *Computer Methods in Applied Mechanics and Engineering* 198(1):2-13. doi:10.1016/j.cma.2008.05.004

Sigmund, O., Maute, K. (2013). Topology optimization approaches: A comparative review. *Structural and Multidisciplinary Optimization* 48(6):1031–1055. doi:10.1007/s00158-013-0978-6

Svanberg, K. (1987). The method of moving asymptotesa new method for structural optimization. *International Journal for Numerical Methods in Engineering* 24(2):359-373. doi:10.1002/nme.1620240207

Tsompanakis, Y., Lagaros, N.D., Papadrakakis, M. (eds) (2008). Structural design optimization considering uncertainties, structures & infrastructures series, vol 1. Taylor & Francis, New York.

Wasiutynski, Z. (1939). Strength design. Part I: Methods of strength design. Part II: Design for minimum potential. Part III: On the design of I-beams. Akademia Nauk Technicznych, Warsaw.

Yin, L., Ananthasuresh, G.K. (2003). Design of Distributed Compliant Mechanisms. *Mechanics Based Design of Structures and Machines* 31(2):151–179. doi:10.1081/SME-120020289

Zhang, J., Wang, B., Niu, F., Cheng, G. (2015). Design optimization of connection section for concentrated force diffusion. *Mechanics Based Design of Structures and Machines* 43(2):209–231. doi:10.1080/15397734.2014.942816

Zhou, M., Lazarov, B. S., Wang, F., Sigmund, O. (2015). Minimum length scale in topology optimization by geometric constraints. *Computer Methods in Applied Mechanics and Engineering* 293:266–282. doi:10.1016/j.cma.2015.05.003